IEEE Access
Multidisciplinary | Rapid Review | Open Access Journal

Received July 11, 2019, accepted July 21, 2019, date of publication July 24, 2019, date of current version August 30, 2019.

Digital Object Identifier 10.1109/ACCESS.2019.2930829

Study on Characteristic Parameters of Short-Circuit Impedance for a Four-Winding Inductive Filtering Transformer in Power System Supplying Nonlinear Loads

ZHAO HUANG[1], YUEHUI CHEN[2], SAIMEI SHI[3], AND LONGFU LUO[1], (Member, IEEE)

[1]College of Electrical and Information Engineering, Hunan University, Changsha 410082, China
[2]State Grid Hunan Electric Power Company, Changsha 410012, China
[3]Hunan Provincial Key Laboratory of Grids Operation and Control on Multi-Power Source Area, Shaoyang University, Shaoyang 422004, China

Corresponding author: Longfu Luo (llf@hnu.edu.cn)

This work was supported in part by the Hunan Province Key Research and Development Project under Grant 2017GK2240, in part by the State Grid Hunan Electric Power Company Technology Project under Grant 5216k0170002, and in part by the Hunan Science and Technology Project of China under Grant 2016TP1023.

ABSTRACT Different from a three-winding transformer and ac passive filtering method, this paper proposes an inductive filtering (IF) method with a four-winding inductive filtering transformer (FW-IFT) for power system supplying nonlinear loads. Based on this, the characteristic parameters of the short-circuit impedance for the FW-IFT are studied in detail by theoretical analysis and experimental verification. According to the single-phase equivalent circuit, the voltage equations of the FW-IFT are established at the fundamental and harmonic frequencies. By short-circuit test, the constraint condition of the inductive filtering is obtained, which can satisfy the demand of nonlinear loads in power system. Then, the influences of the filter impedance on characteristic parameter of the short-circuit impedance are analyzed and calculated. The detailed theoretical calculation and the experimental results verified the feasibility and correctness of the aforementioned theoretical analysis and calculation.

INDEX TERMS Four-winding inductive filtering transformer, inductive filtering, short-circuit impedance, equivalent circuit, theoretical analysis.

I. INTRODUCTION

A three-winding transformer is a key electrical equipment in power systems supplying nonlinear loads. The Increasing use of nonlinear loads creates harmonic distortion at the utility grid, which is transmitted from the load side to the utility grid side by three-winding transformer. This harmonic distortion gives rise to overheating of transformer, higher line losses, and derating reactive power [1]–[5]. Additionally, these current harmonic interactions between the utility grid and loads lead to voltage harmonics, and finally, safe operating and system stability problems in the power system. So, the power quality of the utility grid, due to current harmonics, has become a major problem at the system voltage level.

Hence, the harmonic reduction techniques are very important to enhance the power quality of the utility grid. There are a variety of harmonic reduction techniques to enhance grid current and voltage waveforms, and which are commonly categorized as passive filtering techniques, active filtering techniques, and hybrid active filtering techniques. Passive filtering techniques with inductance (L) and capacitor (C) are preferred because of their simplicity, economical cost, and reliability. However, passive filters are easily to occur series and/or parallel resonances between system impedance and filter impedance, which make harmonic amplification [6], [7]. Active filtering techniques which are usually made of a three-phase voltage inverter with a dc-link capacitor also limit the flow of current harmonics into the utility grid [8]–[11]. Hybrid active filtering techniques composed of an active filter with passive filter can prevent current harmonics into the utility grid [12]–[15]. However, two later techniques are not suitable for a high-power and high-voltage level of the power system to eliminate current harmonics due to capacity limitation of the inverter and the complexity of the control algorithm.

The associate editor coordinating the review of this manuscript and approving it for publication was Firuz Zare.

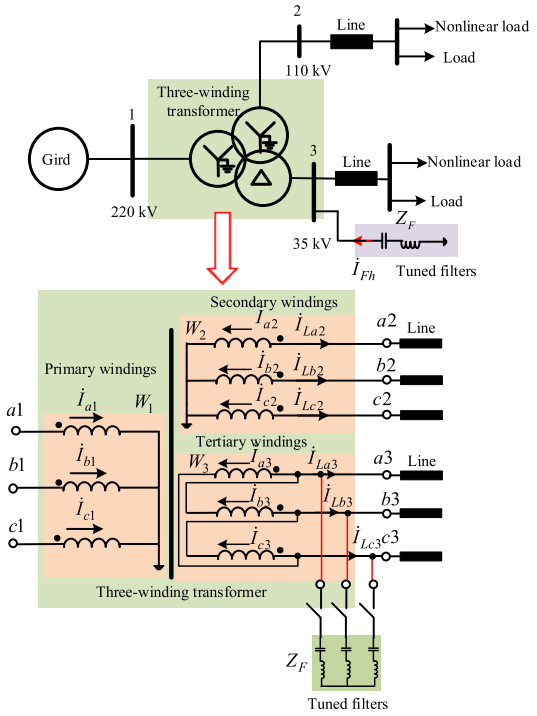

FIGURE 1. Wiring scheme of three-winding transformer and passive filtering method.

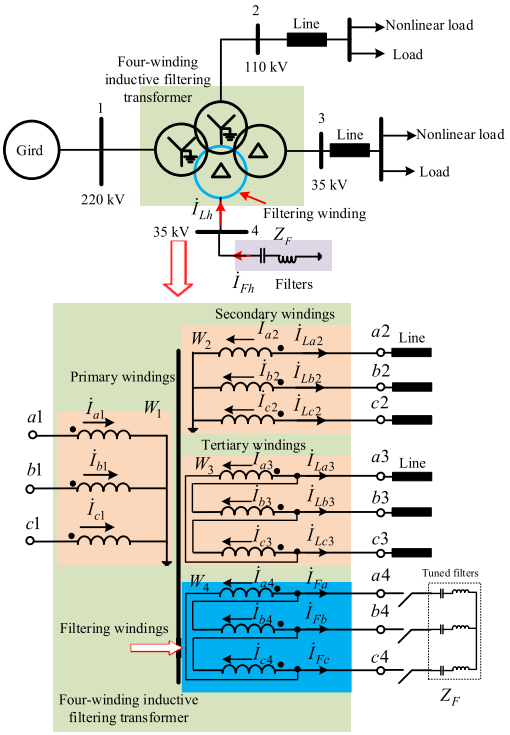

FIGURE 2. Wiring scheme of four-winding inductive filtering transformer and corresponding inductive filtering system.

Therefore, the inductive filtering method with a four-winding inductive filtering transformer (FW-IFT) is presented to shield load current harmonics into the utility grid. Different from the other papers' investigating contents, the aim of this paper is further to study on the characteristic parameters of short-circuit impedance for the FW-IFT and the inductive filtering approach, which are concerned with the prototype of the FW-IFT in experiment.

II. SYSTEM STRUCTURE DESCRIPTION

Fig.1 and Fig.2 present the three-winding transformer and passive filtering method, and the four-winding inductive filtering transformer and the tuned filtering circuit for inductive filtering, respectively. Note that the FW-IFT has an independent filtering winding, which a linking point of the filtering winding connected with passive filters acts as the filtering system implementing inductive filtering at harmonic frequencies.

A. INFLUENCE OF LOAD HARMONIC ON THE UTILITY GRID

A conventional power system mainly consists of power supply source, three-winding transformer, transmission line, passive filters, and power loads, as shown in Fig.1. Provided that current harmonics generated by nonlinear loads are of $6k \pm 1$(k is the integer) order characteristics. These characteristic current harmonics will deliver into the utility grid by the three-winding transformer, which make the same harmonic component of $6k \pm 1$ order characteristics. Therefore, the traditional filtering scheme is that passive filters are always placed in tertiary winding or low-voltage side of this transformer. In such a scheme, the passive filtering method can only alleviate harmonics of the low-voltage (LV) load side, whilst it cannot reduce that of the medium-voltage (MV) load side, and thus the power quality of the utility grid or high-voltage (HV) supply terminal cannot satisfy the IEEE Standard 519 [16].

Therefore, an inductive filtering method with a FW-IFT is proposed to apply in power system supplying nonlinear loads, as illustrated in Fig.2. The FW-IFT is designed according to the equivalent zero impedance principle, which makes the filtering winding as filtering path. The equivalent calculated impedances of the filtering winding are closely equal to zero, and the impedance of the passive filters is zero at the special frequency. Once two conditions are matched, the inductive filtering technique will be implemented. In such a way, the main characteristic harmonics generated by nonlinear loads of the MV and/or LV side can be shielded, meanwhile the harmonic magnetic potential of the transformer can be decreased greatly, and there are few current harmonics at the utility grid, which implies that the bad influences of the harmonic and reactive power on the FW-IFT can be alleviated immensely.

B. SHORT-CIRCUIT IMPEDANCE OF THE FW-IFT

Short-circuit impedance of transformer is of greatly important characteristic parameters for the operation of power system supplying nonlinear loads [17]–[19], especially for the FW-IFT, which directly influences its filtering performance and the capability of reactive power compensation.

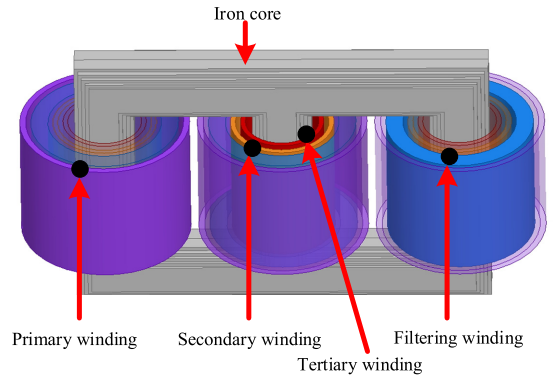

FIGURE 3. Winding structure of the FW-IFT.

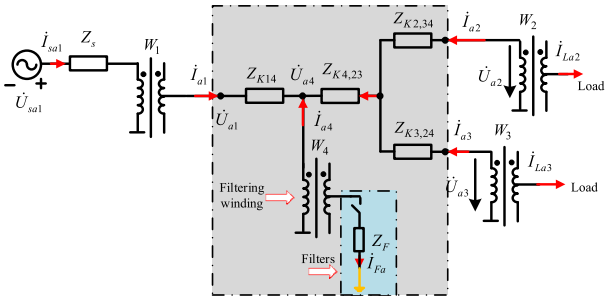

FIGURE 4. Single-phase equivalent circuit of the FW-IFT.

As for the three-winding transformer shown in Fig.1, this transformer adopts wye/wye/delta-connected winding, and corresponding short-circuit impedance parameter has been reported in the literatures [20], [21].

As for wiring scheme and winding structure of the FW-IFT, respectively, shown in Fig.2 and Fig. 3, there has four windings, such as the wye-connected primary winding, the wye-connected secondary winding, the delta-connected tertiary winding, and the delta-connected filtering winding. In the meantime, the equivalent calculated impedance of the filtering winding is designed to closely zero (by ignoring resistor of the transformer) according to the equivalent zero impedance principle. This designed structure ensures that the impedance of the filtering branch is approximately equal to 0 at the harmonic frequency, which is provided a filtering path for realizing the inductive filtering. The symmetrical configuration ensures that the each-phase short-circuit impedance of the FW-IFT is equal, which implies that the error of short-circuit impedance is simply controlled. Also, the equal of each-phase impedance can confirm the symmetry of the FW-IFT configuration, which is a merit of the normal operation and to implement the inductive filtering.

III. THEROTICAL ANALYSIS OF CHARACTERISTIC PARAMETERS

Fig.4 shows single-phase equivalent circuit of the FW-IFT which is of four nodes and branches. Since the equivalent calculated impedance of the filtering winding is 0, this equivalent circuit is a radiation-connected circuit which includes one short-circuit impedance Z_{K14} and three equivalent calculated impedances $Z_{K2,34}$, $Z_{K3,24}$, $Z_{K4,23}$. The operating characteristics of the FW-IFT are described from this equivalent circuit: 1) Assumed that load harmonics do not occur in the MV and LV sides, without passive filters, the function of the FW-IFT is similar to three-winding transformer; 2) Assumed that power factor of the utility grid is lower than 0.9 in 1) scenario, reactive power compensation will be performed by capacitors connected to the filtering winding, and so it enhances power factor; 3) Assumed that load harmonics occur in the MV and/or LV load sides, harmonics compensation will be implemented by passive filters connected to the filtering winding, and thus it can shield load harmonics. Hence, the short-circuit impedance is very important characteristic parameters for realizing the IF method.

A. VOLATGE EQUATIONS

For the sake of solving the characteristic parameters of the short-circuit impedance for the FW-IFT, the equations which expresses the characteristic of the voltage transfer of the FW-IFT should be established at the first.

Ignoring the excitation current and according to the ampere-turns balance principle, the magnetic balance equation of the FW-IFT can be obtained as

$$\dot{I}_{Fa} = \frac{W_1}{W_4}\sqrt{3}e^{j\frac{\pi}{6}}\dot{I}_{sa1} - \frac{W_2}{W_4}\sqrt{3}e^{j\frac{\pi}{6}}\dot{I}_{La2} - \frac{W_3}{W_4}\dot{I}_{La3} \tag{1}$$

The voltage equation of the filtering winding is expressed as

$$\dot{U}_{Fa} = Z_F\dot{I}_{Fa} \tag{2}$$

Assumption of three-phase symmetric system, the voltage equations of the FW-IFT are obtained as follows

$$\begin{cases} \dot{U}_{sa1} - \dfrac{W_1}{W_4}\sqrt{3}e^{-j\frac{\pi}{6}}\dot{U}_{Fa} = Z_{K14}\dot{I}_{sa1} \\ \dfrac{W_1}{W_2}\dot{U}_{La2} - \dfrac{W_1}{W_4}\sqrt{3}e^{-j\frac{\pi}{6}}\dot{U}_{Fa} = -Z_{K24}\dfrac{W_2}{W_1}\dot{I}_{La2} \\ \quad -Z_{K4,23}\dfrac{W_3}{W_1}\dfrac{1}{\sqrt{3}e^{j\frac{\pi}{6}}}\dot{I}_{La3} \\ \dfrac{W_1}{W_3}\sqrt{3}e^{-j\frac{\pi}{6}}\dot{U}_{La3} - \dfrac{W_1}{W_4}\sqrt{3}e^{-j\frac{\pi}{6}}\dot{U}_{Fa} = -Z_{K4,23}\dfrac{W_2}{W_1}\dot{I}_{La2} \\ \quad -Z_{K34}\dfrac{W_3}{W_1}\dfrac{1}{\sqrt{3}e^{j\frac{\pi}{6}}}\dot{I}_{La3} \end{cases} \tag{3}$$

where, W_m is the number of turns for m-winding of transformer; $\dot{U}_{sa1}$, $\dot{U}_{La2}$, $\dot{U}_{La3}$, and $\dot{U}_{Fa}$ are the phase-a port voltage of primary, secondary, tertiary, and filtering winding of the FW-IFT, respectively; $\dot{I}_{sa1}$, $\dot{I}_{La2}$, $\dot{I}_{La3}$, and $\dot{I}_{Fa}$ are the phase-a port current of primary, secondary, tertiary, and filtering winding of the FW-IFT, respectively; Z_F is the filter impedance. Z_{Kmn} is the short-circuit impedance between m- and n-winding; $Z_{Kk,mn}$ is the equivalent calculated impedance for k-winding among m-, n-, and k-winding; relation between $Z_{Kk,mn}$ and the short-circuit impedances (Z_{Kkm}, Z_{Kkn}, Z_{Kmn}) is $Z_{Kk,mn} = 0.5(Z_{Kkm} + Z_{Kkn} - Z_{Kmn})$; $k, m, n = 1, \cdots, 4$, $k \neq m \neq n$.

TABLE 1. Measures the short-circutimpedance.

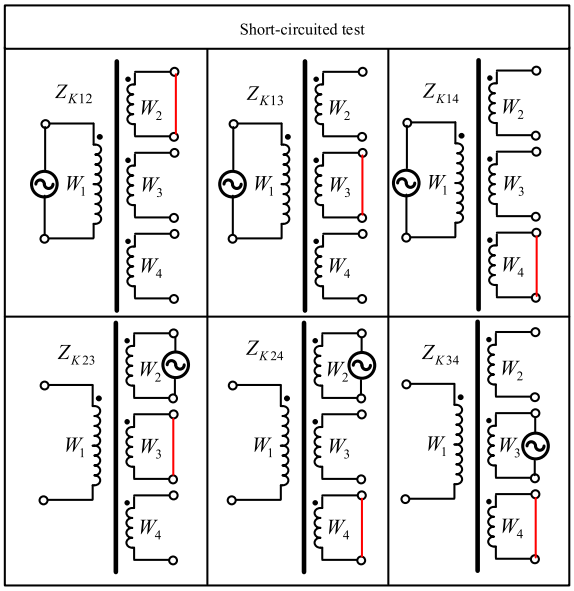

Using (1) and (2) in (3) yields, the voltage equations of winding port for the FW-IFT can be obtained as follows

$$\begin{cases} \dot{U}_{a1} = (Z_{K14} + 3Z_F\dfrac{W_1^2}{W_4^2})\dot{I}_{a1} - 3Z_F\dfrac{W_1W_2}{W_4^2}\dot{I}_{La2} \\ \qquad - Z_F\dfrac{W_1W_3}{W_4^2}\sqrt{3}e^{-j\frac{\pi}{6}}\dot{I}_{La3} \\ \dot{U}_{La2} = 3Z_F\dfrac{W_1W_2}{W_4^2}\dot{I}_{a1} - (3Z_F\dfrac{W_2^2}{W_4^2} + Z_{K24}\dfrac{W_2^2}{W_1^2})\dot{I}_{La2} \\ \qquad - \dfrac{1}{\sqrt{3}e^{j\frac{\pi}{6}}}(3Z_F\dfrac{W_2W_3}{W_4^2} + Z_{K4,23}\dfrac{W_2W_3}{W_1^2})\dot{I}_{La3} \\ \dot{U}_{La3} = \sqrt{3}\,e^{j\frac{\pi}{6}}Z_F\dfrac{W_1W_3}{W_4^2}\dot{I}_{a1} - \dfrac{e^{j\frac{\pi}{6}}}{\sqrt{3}}(3Z_F\dfrac{W_2W_3}{W_4^2} \\ \qquad + Z_{K4,23}\dfrac{W_2W_3}{W_1^2})\dot{I}_{La2} - (Z_F\dfrac{W_3^2}{W_4^2} + Z_{K34}\dfrac{1}{3}\dfrac{W_3^2}{W_1^2})\dot{I}_{La3} \end{cases} \tag{4}$$

From (4), the voltages transfer equations of each port for the FW-IFT at the fundamental and harmonic frequencies are described to derive the characteristic parameters and constraint condition on the short-circuit impedance.

B. CONSTRAINT CONDITION ON THE SHORT-CIRCUIT IMPEDANCE

While winding i is energized, winding j is short-circuited, keeping the remaining windings in open circuit as shown in Table. 1. From this test, the short-circuit impedance between two windings Z_{Kij} is calculated as [22].

$$Z_{Kij} = \left.\frac{U_i}{I_j}\right|_{U_j=0, I_q=0} \qquad i \neq j;\ q \neq i, j;\ i, j,\ q = 1, 2, 3, 4 \tag{5}$$

where, U_i is the voltage source connected to the winding i, I_i is the current flowing through the winding i, I_q is the current flowing through the other windings. This short-circuited test is made for all of the six possible combinations of pairs of windings. The subscript f is denoted as scenario 1 without filters at the fundamental frequency, and the subscript if is denoted as Scenario 2 with filters.

TABLE 2. Measures the short-circuit impedance with filter impedance.

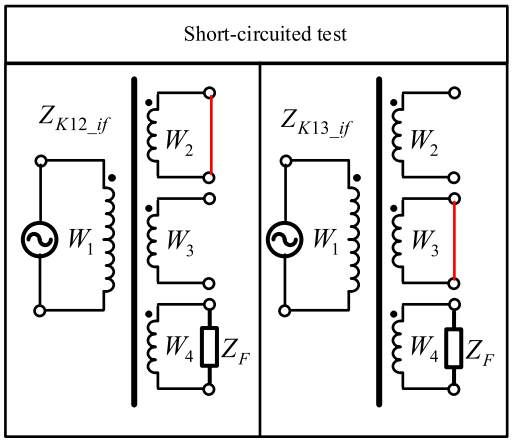

Table 1 shows the six short-circuit impedances (Z_{K12}, Z_{K13}, Z_{K14}, Z_{K23}, Z_{K24}, and Z_{K34}) measured by three-phase short-circuited test. Yet, Table 2 shows the two short-circuit impedances (Z_{K12_if} and Z_{K13_if}) measured by three-phase short-circuited test when the filtering winding connects with passive filter. Meanwhile, the influence of the filter impedance (Z_F) on the short-circuit impedance will be analyzed by comparison of Z_{K12}, Z_{K13} and corresponding Z_{K12_if}, Z_{K13_if}.

1) THEORETICAL ANALYSIS OF Z_{K12}

By symmetric short-circuited test on the MV side, so the following results will satisfy

$$\begin{cases} \dot{U}_{La2} = \dot{U}_{Lb2} = \dot{U}_{Lc2} = 0 \\ \dot{I}_{La3} = \dot{I}_{Lb3} = \dot{I}_{Lc3} = 0 \end{cases} \tag{6}$$

By substituting (6) into (4), then substituting the results are that

$$\begin{cases} \dot{U}_{sa1} = (Z_{K14} + 3Z_F\dfrac{W_1^2}{W_4^2})\dot{I}_{sa1} - 3Z_F\dfrac{W_1W_2}{W_4^2}\dot{I}_{La2} \\ 3Z_F\dfrac{W_1W_2}{W_4^2}\dot{I}_{sa1} = (3Z_F\dfrac{W_2^2}{W_4^2} + Z_{K24}\dfrac{W_2^2}{W_1^2})\dot{I}_{La2} \end{cases} \tag{7}$$

By eliminating intermediate variable $\dot{I}_{La2}$ in (7), so a Z_{K12} can be written as

$$Z_{K12} = \frac{\dot{U}_{sa1}}{\dot{I}_{sa1}} = Z_{K14} + \frac{3Z_FZ_{K24}}{3Z_F + Z_{K24}\frac{W_4^2}{W_1^2}} \tag{8}$$

From (8), the expression of Z_{K12} related two short-circuit impedances (Z_{K14}, Z_{K24}), filter impedance Z_F, and turn ratio between winding number *1* and *4* is described.

Scenario 1: Without filter, such as,$Z_F = \infty$, Z_{K12_f} is obtained as

$$Z_{K12-f} = Z_{K14} + Z_{K24} \tag{9}$$

Scenario 2: With filter, such as,$Z_F \neq \infty$, since the filter impedance is much bigger than the short-circuit impedances of the FW-IFT at the fundamental frequency, the following results can be obtained

$$\begin{cases} 3\,|Z_F| \gg Z_{K24} \\ 3\,|Z_F| \gg Z_{K24}\dfrac{W_4^2}{W_1^2} \end{cases} \tag{10}$$

By substituting (10) into (8), Z_{K12-if} is obtained as

$$Z_{K12-if} \approx Z_{K14} + Z_{K24} \tag{11}$$

2) THEORETICAL aNALYSIS OF Z_{K13}:

Similarly, by symmetric short-circuited test on the LV side, so the following results will satisfy

$$\begin{cases} \dot{I}_{La2} = \dot{I}_{Lb2} = \dot{I}_{Lc2} = 0 \\ \dot{U}_{La3b3} = \dot{U}_{Lb3c3} = \dot{U}_{Lc3a3} = 0 \end{cases} \tag{12}$$

By substituting (12) into (4), then substituting the results are that

$$\begin{cases} \dot{U}_{sa1} = (Z_{K14} + 3Z_F\dfrac{W_1^2}{W_4^2})\dot{I}_{sa1} - Z_F\dfrac{W_1W_2}{W_4^2}\sqrt{3}e^{-j\frac{\pi}{6}}\dot{I}_{La3} \\ \sqrt{3}e^{j\frac{\pi}{6}}Z_F\dfrac{W_1W_3}{W_4^2}\dot{I}_{sa1} = (Z_F\dfrac{W_2W_3}{W_4^2} + Z_{K34}\dfrac{1}{3}\dfrac{W_3^2}{W_1^2})\dot{I}_{La3} \end{cases} \tag{13}$$

By eliminating intermediate variable $\dot{I}_{La3}$ in (13), so Z_{K13} can be written as

$$Z_{K13} = \frac{\dot{U}_{sa1}}{\dot{I}_{sa1}} = Z_{K14} + \frac{3Z_FZ_{K34}}{3Z_F + Z_{K34}\frac{W_4^2}{W_1^2}} \tag{14}$$

From (14), the expression of Z_{K13} related two short-circuit impedances (Z_{K14}, Z_{K34}), filter impedance Z_F, and turn ratio between winding number *1* and *4* is described.

Scenario 1: Without filter, such as $Z_F = \infty$, Z_{K13-f} is obtained as

$$Z_{K13-f} = Z_{K14} + Z_{K34} \tag{15}$$

Scenario 2: With filter, such as $Z_F \neq \infty$, since the filter impedance is much bigger than the short-circuit impedances of the FW-IFT at the fundamental frequency, the following results can be obtained

$$\begin{cases} 3\,|Z_F| \gg Z_{K34} \\ 3\,|Z_F| \gg \dfrac{W_4^2}{W_1^2}Z_{K34} \end{cases} \tag{16}$$

By substituting (16) into (14), Z_{K13-if} is obtained as

$$Z_{K13-if} \approx Z_{K14} + Z_{K34} \tag{17}$$

TABLE 3. Designed parameter of a FW-IFT prototype.

Content	Primary	Secondary	Tertiary	Filtering
Rated capacity (kVA)	10	10	10	10
Rated voltage (V)	380	100	100	220
Rated current (A)	15.19	57.73	57.73	26.31
Number of turn	122	32	55	122
Connection mode	YN	yn0	d11	d11
Winding resistor (Ω)	0.23056	0.01214	0.03037	0.05502

The expression of the equivalent calculated impedance of the filtering winding is that

$$\begin{cases} Z_{K4,12} = 0.5(Z_{K14} + Z_{K24} - Z_{K12}) \\ Z_{K4,13} = 0.5(Z_{K14} + Z_{K34} - Z_{K13}) \end{cases} \tag{18}$$

From (9) and (15), the characteristic parameters of the short-circuit impedance for the FW-IFT will satisfy a certain constraint condition, and the equivalent calculated impedance of the filtering winding was indirectly deduced to be equal to 0, which means that the FW-IFT has a filtering winding. Therefore, the constraint condition of the FW-IFT is both $Z_{K4,12} = 0$ and $Z_{K4,13} = 0$. Similarly, once the FW-IFT meets this constraint condition, it can implement the inductive filtering. With filters, the difference in the selected value of both Z_{K12-if} and Z_{K12-f}, both Z_{K13-if} and Z_{K13-f} is almost equal by comparison of theoretical calculations from (11) and (9), (17) and (15), which shows that both the short-circuit impedances (Z_{K12}, Z_{K13}) and the filter impedance Z_F have not relation directly. Therefore, both the filtering winding and the other windings have only the magnetic relation but no the electrical relation.

So, the characteristic parameters of the short-circuit impedance for the FW-IFT are that

$$\begin{matrix} Z_{K12} & Z_{K13} & Z_{K14} \\ & Z_{K23} & Z_{K24} \\ & & Z_{K34} \end{matrix}$$

$$Constraints: \begin{cases} Z_{K12} = Z_{K14} + Z_{K24} \\ Z_{K13} = Z_{K14} + Z_{K34} \end{cases} \tag{19}$$

From (19), the FW-IFT has six characteristic parameters of short-circuit impedance, such as,Z_{K12}, Z_{K13}, Z_{K14}, Z_{K23}, Z_{K24}, and Z_{K34}, and thus Z_{K12}, Z_{K13} need to satisfy a certain constraint condition. Meanwhile, we confirm if this transformer is a FW-IFT from this constraint condition.

IV. EXPERIMENTAL VERIFICATION

A. DESCRIPTION OF SHORT-CIRCUIT TEST

The prototype of a FW-IFT based on the equivalent zero impedance principle is designed, which the designed parameters are shown in Table 3. Fig.5 shows the short-circuited test to measure the characteristic parameters of the short-circuit impedances for the FW-IFT. This test is made of the FW-IFT, supply transformer, and experimental platform, and while double arm bridge apparatus is used to measure resistance

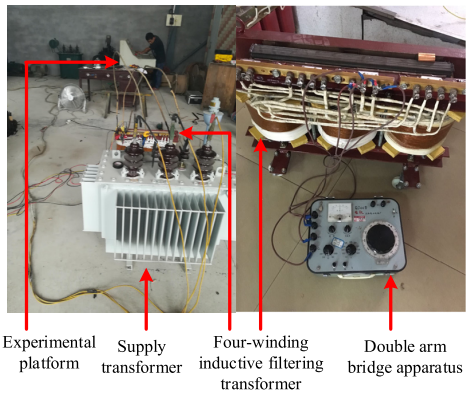

FIGURE 5. Short-circuited test of the FW-IFT prototype.

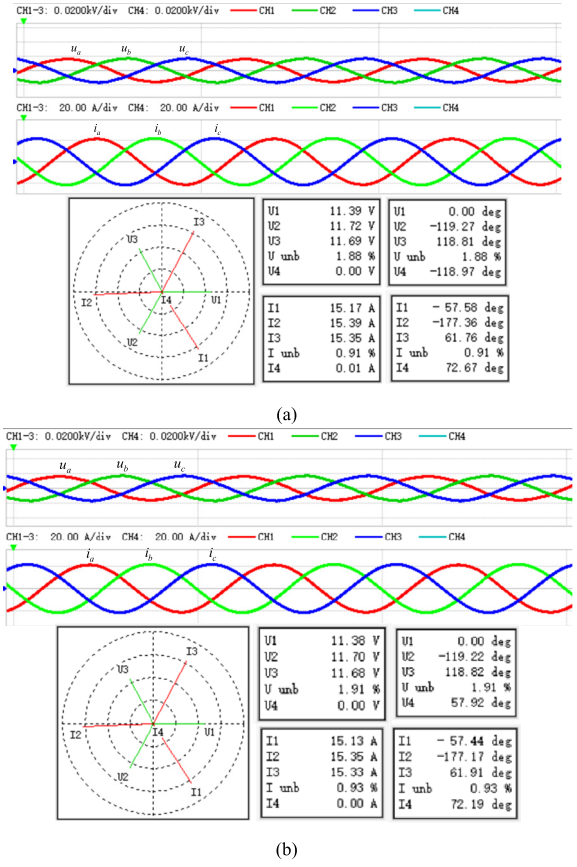

FIGURE 6. Waveforms and phasor diagram of three-phase voltages and currents when measured Z_{K12}. (a) Without filter. (b) With filter.

of FW-IFT. It adopts the 11th-order passive filter, which the inductor (L_F) and capacitor (C_F) are 3 mH and 28 μ F, respectively, and so the filter impedance Z_F is $-$j112.8 Ω at the fundamental frequency.

The characteristic parameters of the short-circuit impedances can be obtained by the short-circuited test as shown in Table 1. The measurements are performed by taking two windings at a time. One winding is energized with a second winding that is short-circuited while keeping the third and fourth winding open. Without filters, the short-circuit impedances, such as, Z_{K12}, Z_{K13}, Z_{K14}, Z_{K23}, Z_{K24}, Z_{K34}, of transformer can be measured by short-circuit test.

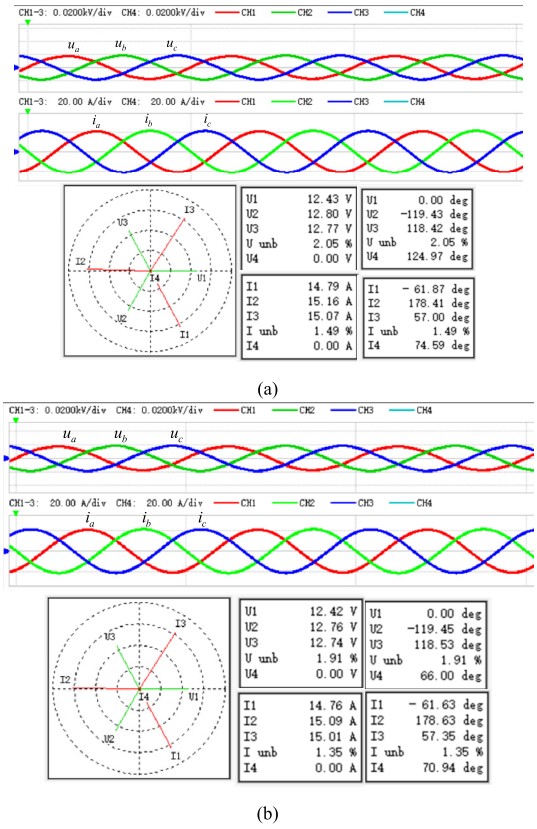

FIGURE 7. Waveforms and phasor diagram of three-phase voltages and currents when measured Z_{K13}. (a) Without filter. (b) With filter.

B. EXPERIMENTAL RESULTS

Experimental results were obtained by short-circuited test for the FW-IFT working as on no-load. Fig.6 (a) shows waveforms and phasor diagram of three-phase voltages and currents when measured short-circuit impedance Z_{K12} without filters ($Z_F = \infty$). Fig.6 (b) shows waveforms and phasor diagram of three-phase voltages and currents when measured short-circuit impedance Z_{K12_if} with filters ($Z_F = -j112.8\Omega$).

Fig.7 (a) shows waveforms and phasor diagram of three-phase voltages and currents when measured short-circuit impedance Z_{K13} without filters ($Z_F = \infty$). Fig.7 (b) shows waveforms and phasor diagram of three-phase voltages and currents when measured short-circuit impedance Z_{K13_if} with filters ($Z_F = -j112.8\Omega$). Table 4 shows the comparison of short-circuit impedances from both the theoretical calculation and experimental results. It can be seen from Table 4 that the theoretical calculation results are the same as the experimental results. Moreover, the results show that the filter impedance at fundamental frequency has no effect on characteristic parameters of the short-circuit impedances Z_{K12}, Z_{K13}.

C. EXPERIMENTAL ANALYSIS

For purpose of verifying the feasibility of the theoretical analysis and describing the harmonic suppression characteristic

TABLE 4. Comparasion of the short-circuit impedance.

	Test	Short-circuit impedance (%) Theoretical calculation	Experimental results
Z_{K14}	$Z_F=\infty$	2.838∠45.8°	2.840∠45.9°
Z_{K23}	$Z_F=\infty$	2.314∠15.5°	2.312∠15.6°
Z_{K24}	$Z_F=\infty$	2.266∠45.4°	2.265∠45.3°
Z_{K34}	$Z_F=\infty$	2.767∠59.7°	2.765∠59.8°
Z_{K12}	$Z_F=\infty$	5.104∠45.6°	5.103∠45.7°
	Z_F=-j112.8Ω	5.105∠45.6 °	5.106∠45.7 °
Z_{K13}	$Z_F=\infty$	5.563∠52.8 °	5.564∠52.8 °
	Z_F=-j112.8Ω	5.565∠52.7 °	5.566∠52.8 °

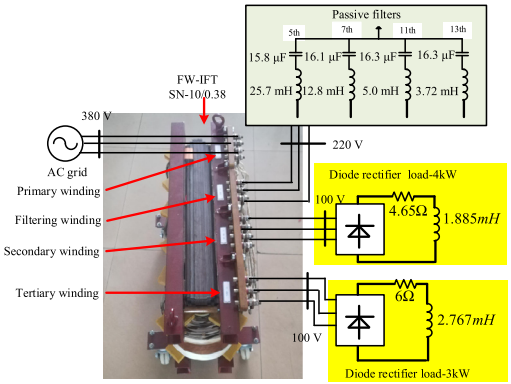

FIGURE 8. Schematic diagram of experimental prototype.

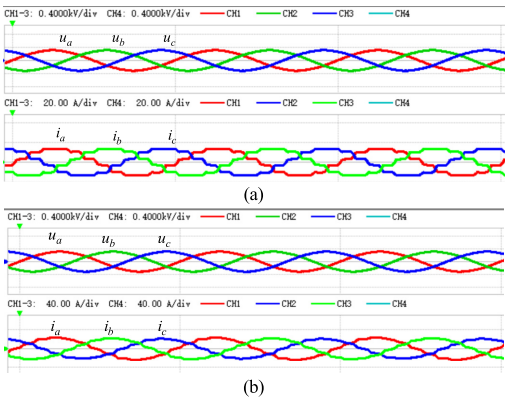

FIGURE 9. Voltage and current experimental waveforms at the 380-V bus. (a) Without filter. (b) With filter.

that FW-IFT has, we established the schematic diagram of the experimental prototype shown in Fig.8 in which includes the FW-IFT, two sets of diode rectifier system as nonlinear loads, passive filters with the 5th, 7th, 11th, and 13th order harmonic. Fig.9 shows the voltage and current experimental waveforms at the 380-V bus both without filters and with filters. Fig.10 shows phase-a current spectra at the 380-V by comparison of both without filters and with filters. It can be seen that the current experimental waveforms at the 380-V bus are approximate to the ideal sine wave, when the implementation of the inductive filtering technique in the filtering winding of the FW-IFT. Since the main characteristic

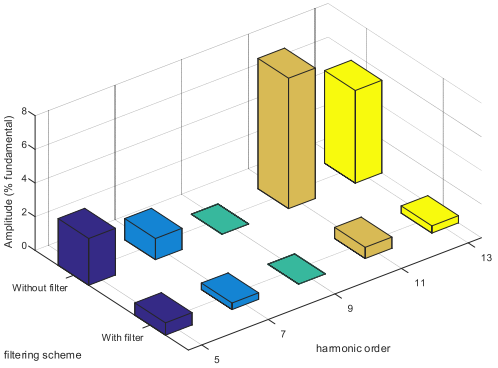

FIGURE 10. Current spectra at the 380-V bus.

harmonics of nonlinear loads have been eliminated in the filtering winding, there are few current harmonics at the utility grid of the FW-IFT, which implies that the filtering system will induce the main current harmonics to offset load current harmonics.

V. CONCLUSION

The characteristic parameters of the short-circuit impedance for the FW-IFT are studied in detail by the systematic analysis and the short-circuited test. The conclusion can be summarized as follows.

1) This paper has set up the constraint relationship of characteristic parameters of the short-circuit impedance for the FW-IFT, deduced by the short-circuited test according to the voltage transfer equations, and then revealed the special independent filtering winding that the FW-IFT has.

2) The equivalent calculated impedance of the filtering winding is indirectly deduced to be closely equal to 0 from the constraint relationship of characteristic parameters of the short-circuit impedance, and the provided a filtering path for implementing inductive filtering.

3) This paper has presented a simple but practical calculation method for characteristic parameters of the short-circuit impedance for the FW-IFT, and further studied that the filter impedance at fundamental frequency has no effect on characteristic parameters of the short-circuit impedance for the FW-IFT.

4) Between the theoretical calculation and experimental results are basically consistent with the theoretical analysis, which proves the feasibility of the theoretical analysis. The experimental results show that the application of the FW-IFT and the inductive filtering method can greatly decreased the load current harmonics in the filtering winding of the FW-IFT.

The leakage inductance matrix of the FW-IFT will be investigated in the further.

REFERENCES

[1] E. Durna, I. Yilmaz, and M. Ermiş, "Suppression of time-varying interharmonics produced by medium-frequency induction melting furnaces by a HAPF system," *IEEE Trans. Power Electron.*, vol. 32, no. 2, pp. 1030–1043, Feb. 2017.

[2] S. H. E. A. Aleem, A. F. Zobaa, and M. M. A. Aziz, "Optimal *C*-type passive filter based on minimization of the voltage harmonic distortion for nonlinear loads," *IEEE Trans. Ind. Electron.*, vol. 59, no. 1, pp. 281–288, Jan. 2012.
[3] J. K. Phipps, "A transfer function approach to harmonic filter design," *IEEE Ind. Appl. Mag.*, vol. 3, no. 2, pp. 68–82, Mar. 1997.
[4] F. Zare, H. Soltani, D. Kumar, P. Davari, H. A. M. Delpino, and F. Blaabjerg, "Harmonic emissions of three-phase diode rectifiers in distribution networks," *IEEE Access*, vol. 5, pp. 2819–2833, 2017.
[5] D. A. Gonzalez and J. C. McCall, "Design of filters to reduce harmonic distortion in industrial power systems," *IEEE Trans. Ind. Appl.*, vol. IA-23, no. 3, pp. 504–512, May 1987.
[6] A. F. Zobaa and A. Aziz, "LC compensators based on transmission loss minimization for nonlinear loads," *IEEE Trans. Power Del.*, vol. 19, no. 4, pp. 1740–1745, Oct. 2004.
[7] L. Wang, C.-S. Lam, and M.-C. Wong, "Multifunctional hybrid structure of SVC and capacitive grid-connected inverter (SVC//CGCI) for active power injection and nonactive power compensation," *IEEE Trans. Ind. Electron.*, vol. 66, no. 3, pp. 1660–1670, Mar. 2019.
[8] S. P. Litrán and P. Salmerón, "Reference voltage optimization of a hybrid filter for nonlinear load compensation," *IEEE Trans. Ind. Electron.*, vol. 61, no. 6, pp. 2648–2654, Jun. 2014.
[9] Y. Wang, J. Xu, L. Feng, and C. Wang, "A novel hybrid modular three-level shunt active power filter," *IEEE Trans. Power Electron.*, vol. 33, no. 9, pp. 7591–7600, Sep. 2018.
[10] J. C. Alfonso-Gil, E. Pérez, C. Ariño, and H. Beltran, "Optimization algorithm for selective compensation in a shunt active power filter," *IEEE Trans. Ind. Electron.*, vol. 62, no. 6, pp. 3351–3361, Jun. 2015.
[11] M. Angulo, D. A. Ruiz-Caballero, J. Lago, M. L. Heldwein, and S. A. Mussa, "Active power filter control strategy with implicit closed-loop current control and resonant controller," *IEEE Trans. Ind. Electron.*, vol. 60, no. 7, pp. 2721–2730, Jul. 2013.
[12] S. Rahmani, N. Mendalek, and K. Al-Haddad, "Experimental design of a nonlinear control technique for three-phase shunt active power filter," *IEEE Trans. Ind. Electron.*, vol. 57, no. 10, pp. 3364–3375, Oct. 2010.
[13] E. Lei, X. Yin, Z. Zhang, and Y. Chen, "An improved transformer winding tap injection DSTATCOM topology for medium-voltage reactive power compensation," *IEEE Trans. Power Electron.*, vol. 33, no. 3, pp. 2113–2126, Mar. 2018.
[14] S. Rahmani, A. Hamadi, N. Mendalek, and K. Al-Haddad, "A new control technique for three-phase shunt hybrid power filter," *IEEE Trans. Ind. Electron.*, vol. 56, no. 8, pp. 2904–2915, Aug. 2009.
[15] T. Lee, Y. Wang, J. Li, and J. M. Guerrero, "Hybrid active filter with variable conductance for harmonic resonance suppression in industrial power systems," *IEEE Trans Ind. Electron.*, vol. 62, no. 2, pp. 746–756, Feb. 2015.
[16] *IEEE Recommended Practice and Requirements for Harmonic Control in Electric Power Systems*, IEEE Standard 519-1992, 2014.
[17] B. Kasztenny and E. Rosolowski, "Modeling and protection of hexagonal phase-shifting transformers—Part I: Short-circuit model," *IEEE Trans. Power Del.*, vol. 23, no. 3, pp. 1343–1350, Jul. 2008.
[18] J. H. Teng, "Unsymmetrical short-circuit fault analysis for weakly meshed distribution systems," *IEEE Trans. Power Syst.*, vol. 25, no. 1, pp. 96–105, Feb. 2010.
[19] J.-H. Teng, "A direct approach for distribution system load flow solutions," *IEEE Trans. Power Del.*, vol. 18, no. 3, pp. 882–887, Jul. 2003.
[20] Y. Li, F. Yao, Y. Cao, W. Liu, F. Liu, S. Hu, L. Luo, Z. Zhang, Y. Chen, G. Zhou, and C. Rehtanz, "An inductively filtered multiwinding rectifier transformer and its application in industrial DC power supply system," *IEEE Trans. Ind. Electron.*, vol. 63, no. 7, pp. 3987–3997, Jul. 2016.
[21] Y. Chen, Z. Huang, Z. Duan, P. Fu, G. Zhou, and L. Luo, "A four-winding inductive filtering transformer to enhance power quality in a high-voltage distribution network supplying nonlinear loads," *Energies*, vol. 12, no. 10, p. 2021, May 2019. doi: 10.3390/en12102021.
[22] C. Alvarez-Marino, F. de Leon, and X. M. Lopez-Fernandez, "Equivalent circuit for the leakage inductance of multiwinding transformers: Unification of terminal and duality models," *IEEE Trans. Power Del.*, vol. 27, no. 1, pp. 353–361, Jan. 2012.